

Unifying KV Cache Compression for Large Language Models with LeanKV

Yanqi Zhang^{1*} Yuwei Hu^{1*} Runyuan Zhao¹ John C.S. Lui² Haibo Chen³
¹Huawei ²The Chinese University of Hong Kong ³Shanghai Jiao Tong University

ABSTRACT

Large language models (LLMs) demonstrate exceptional performance but incur high serving costs due to substantial memory demands, with the key-value (KV) cache being a primary bottleneck. Existing KV cache compression methods, including quantization and pruning, struggle with limitations such as uniform treatment of keys and values and static memory allocation across attention heads. To address these challenges, we introduce LeanKV, a unified KV cache compression framework that enhances LLM serving efficiency without compromising accuracy through three innovations: (1) Hetero-KV quantization, which stores keys at a higher precision than values to reflect their greater impact on attention computations; (2) per-head dynamic sparsity, which allocates memory based on token importance per head and per request; and (3) unified KV compression, integrating mixed-precision quantization and selective pruning to enable a smooth tradeoff between model accuracy and memory efficiency. To efficiently support these techniques, LeanKV introduces systems optimizations including unified paging and on-GPU parallel memory management. Implemented on vLLM, LeanKV compresses the KV cache by 3.0× to 5.0× without accuracy loss and up to 11.0× with under 5% accuracy loss, enhancing throughput by 1.9× to 2.5×, and up to 6.9×.

1 INTRODUCTION

Large language models (LLMs) like GPT [4, 7, 43] and Gemini [52] have demonstrated significant potential to impact our daily lives, offering promising applications in areas including chatbots [10, 53], programming [21, 23], mathematics [47, 64] and medical assistance [46, 58]. Despite their exceptional performance, hosting LLMs is costly due to their large model sizes, demanding extensive hardware resources. Given the pervasive adoption of LLMs, enhancing serving efficiency has become critically important [6, 16, 24, 29, 33, 44, 50, 61].

LLMs are fundamentally based on the Transformer architecture [55, 56], which employs the attention mechanism to generate tokens sequentially, based on the input prompt and previously generated tokens. Within the attention mechanism, each token is transformed into query, key and value feature vectors. The attention scores, derived from the dot product

of the query and key vectors, enable the model to weigh the significance of different tokens. Subsequently, the output is computed as the weighted sum of the value vectors, based on the attention scores. To capture diverse relationships between tokens, the attention mechanism is typically divided into multiple heads [5, 48, 55]. Each head independently computes attention, and their outputs are concatenated and transformed to create a richer representation of the input data

To avoid redundant computation, LLM inference frameworks typically cache intermediate key and value tensors in memory, commonly referred to as the KV cache [30]. The size of the KV cache scales linearly with both sequence length and the number of concurrent requests, often comprising over 90% of total memory consumption [19, 30, 59, 60]. As state-of-the-art models continue to support longer sequences [4, 15, 28, 36, 52, 54], the KV cache has emerged as a critical bottleneck for LLM serving efficiency. It limits the number of concurrent requests that can fit in memory and increases attention computation latency due to its memory bandwidth-bound nature [12, 13].

Recognizing the critical role of the KV cache in limiting serving efficiency, researchers have investigated various compression techniques, primarily focused on quantization [2, 26, 35] and pruning [8, 20, 32, 57, 62]. Quantization reduces the size of the KV cache by converting floating-point feature values into integers, representing them based on pre-defined intervals. Pruning, on the other hand, reduces the token sequence length by eliminating tokens deemed insignificant based on attention scores. Despite the promise of these techniques, both of them face limitations in efficiency and practicality. First and foremost, existing quantization methods apply the same treatment to key and value vectors of all tokens, disregarding the different roles of keys and values in attention computation, as well as the varying significance of different tokens. Second, current pruning methods statically allocate memory across attention heads, failing to account for the dynamic attention patterns across heads and requests. Moreover, these pruning methods have not been comprehensively evaluated on workloads requiring advanced reasoning, such as programming and mathematics. Lastly, prior work has largely overlooked the potential of unifying quantization and pruning to achieve even greater serving efficiency.

*Equal contribution.

In this paper, we propose *LeanKV*, a unified KV cache compression framework that addresses the limitations of existing methods and enhances LLM serving efficiency. LeanKV introduces three algorithmic principles:

1. Hetero-KV. LeanKV compresses key and value vectors using heterogeneous precisions, with key vectors stored at higher precision and value vectors at lower precision. This design leverages the observation that key vectors have a greater influence on attention calculations, as they affect the attention scores of all tokens, whereas value vectors only impact the contributions of individual tokens to the attention output.

2. Per-head Dynamic Sparsity. LeanKV dynamically identifies critical tokens on a per-head and per-request basis, adjusting memory allocation accordingly. This design stems from the observation that attention score distributions exhibit dynamic sparsity across both heads and requests. Within a single request, the number of critical tokens varies across heads, and for the same head, the number of critical tokens also varies across different requests.

3. Unified KV Compression. Built on Hetero-KV quantization and per-head dynamic sparsity, LeanKV unifies KV compression strategies by applying mixed-precision quantization and selective pruning on a per-head and per-request basis, with token importance serving as a unified metric. Critical tokens are stored at higher precision, less important tokens are quantized at lower precision, and the least significant tokens are pruned. This integrated approach enables a smooth tradeoff between model accuracy and memory efficiency.

Implementing LeanKV’s algorithmic innovations presents new challenges in system design, particularly regarding memory management. Unlike traditional attention mechanisms that adopt uniform memory allocation across attention heads, LeanKV requires dynamic, per-head memory allocation for each request, significantly increasing system complexity. Moreover, LeanKV must flexibly configure memory to accommodate varying numbers of tokens stored at different precision levels or pruned entirely, further complicating memory management.

To address these challenges, LeanKV introduces two novel techniques. First, LeanKV employs *unified paging*, which divides memory into fixed-size pages containing vectors stored at various precisions. Each page is dynamically parsed based on the precision configuration required by the head and request, while an attention GPU kernel is co-designed with the page layout to maximize memory bandwidth utilization. Second, LeanKV introduces an *on-GPU memory management* mechanism that accelerates memory management by parallelizing it directly on the GPU with minimal metadata overhead.

We implement LeanKV on vLLM [30], a state-of-the-art LLM inference system, and evaluate it across three prominent model families using representative workloads, including

tasks that demand advanced reasoning such as mathematics and coding. Our experimental results demonstrate that LeanKV offers a superior cost-accuracy tradeoff compared to existing KV cache management methods. Specifically, LeanKV compresses the KV cache by 3.0× to 5.0× without loss in model accuracy, and by up to 11.0× with a marginal accuracy reduction of under 5%, resulting in throughput improvement of 1.9× to 2.5×, and up to 6.9× correspondingly.

2 BACKGROUND AND RELATED WORK

In this section, we describe Transformer-based large language models and review existing techniques for KV cache management aimed at improving LLM serving efficiency.

2.1 Large Language Models

Transformer Architecture. Large language models (LLMs) are predominantly built upon the Transformer architecture [55], which is used to capture complex long-range dependencies in sequential data. At the core of Transformer architecture is the attention mechanism, which allows each token in a sequence to weigh the significance of other tokens when constructing its contextualized representation. Mathematically, the attention computation is defined as:

$$\begin{aligned} \text{Attention}(\mathbf{Q}, \mathbf{K}, \mathbf{V})_i &= \sum_{j=1}^i \text{softmax} \left(\frac{\mathbf{Q}\mathbf{K}^\top}{\sqrt{d}} \right)_{ij} \mathbf{v}_j \\ &= \sum_{j=1}^i \frac{\exp \left(\frac{\mathbf{q}_i \cdot \mathbf{k}_j}{\sqrt{d}} \right)}{\sum_{n=1}^i \exp \left(\frac{\mathbf{q}_i \cdot \mathbf{k}_n}{\sqrt{d}} \right)} \mathbf{v}_j \end{aligned} \quad (1)$$

\mathbf{Q} and \mathbf{K} are matrices of size $l \times d$, representing the queries and keys, respectively, where l denotes the number of tokens and d represents the feature dimensionality. Vectors \mathbf{q}_i , \mathbf{k}_i , and \mathbf{v}_i correspond to the query, key, and value of the i^{th} token. The dot product between \mathbf{Q} and \mathbf{K} measures the relevance between each pair of query and key. The softmax function normalizes these dot products to form a probability distribution, referred to as attention scores, which are used to compute a weighted sum of the value vectors and produce the output.

To capture a broader range of interactions between tokens, Transformer models employ multi-head attention (MHA), where each head independently computes attention using distinct projections of queries, keys, and values. The outputs from different heads are concatenated and linearly transformed to create a more expressive representation. Grouped-query attention (GQA) [5] improves the efficiency of MHA by allowing a group of query heads to share the same projection of keys and values, referred to as a KV head.

Autoregressive Generation and KV Cache. The autoregressive generation process of LLMs consists of two phases: the *prompt phase*, during which the model computes latent representations for all tokens in the *prompt*, the user-provided

context, and generates the first new token, and the *generation phase*, where the model iteratively generates subsequent tokens by attending to both the prompt and previously generated tokens. To avoid redundant computations across generation steps, *KV cache* is introduced to store the keys and values of all previous tokens. However, the size of the KV cache grows linearly with both the sequence length and batch size, quickly becoming a bottleneck for inference throughput [30, 60]. Therefore, efficient KV cache management is critical for alleviating memory bottlenecks and improving LLM serving efficiency.

2.2 KV Cache Optimization

PagedAttention. Static KV cache management systems [1, 60] reserve memory for the maximum possible sequence length, leading to considerable memory waste when actual sequences are shorter. To mitigate this inefficiency, vLLM [30] introduces *PagedAttention*, which partitions the KV cache into pages, each containing a fixed number of tokens, and allocates the pages on-demand as the sequence length grows. By managing the KV cache at the granularity of pages, vLLM reduces memory waste and enables larger batch sizes to improve serving efficiency.

KV Cache Quantization. Quantization [14, 22, 26, 39] reduce the KV cache size by approximating high-precision floating points with discrete low-bit values. To quantize a given tensor \mathbf{X} , we first calculate the scale s and zero point z as shown in Eq. (2), where X_{\max} and X_{\min} represent the maximum and minimum values in \mathbf{X} , and b is the bit-width. Then, quantization is applied element-wise as: $\mathbf{Q} = \text{round}(\frac{\mathbf{X}+z}{s})$. During inference, the original values are approximately reconstructed via dequantization: $\hat{\mathbf{X}} = s \cdot \mathbf{Q} - z$. Unlike the quantized tensor \mathbf{Q} , the metadata s and z are kept in higher precision (e.g., FP16) to ensure more accurate dequantization.

$$s = \frac{X_{\max} - X_{\min}}{2^b - 1}, \quad z = -X_{\min} \quad (2)$$

State-of-the-art KV cache quantization methods such as Atom [63] and Qserve [35] apply this process to each key and value vector independently. However, these uniform quantization methods, which apply a fixed bit-width across keys and values of all tokens, may not be optimal. They overlook the varying importance of tokens as well as the different roles of keys and values in the attention calculation.

KV Cache Pruning. Several recent works [8, 20, 32, 37, 57, 62] have explored KV cache pruning to alleviate the memory bottleneck in LLM inference, which can be considered as an extreme case of quantization. These methods use attention scores to assess token importance and evict less important tokens, thereby reducing the KV cache size. The effectiveness of these methods, however, is limited by their static and inflexible allocation of memory resources. Specifically, H2O [62]

and SnapKV [32] allocate the same memory budget uniformly across all attention heads and layers. PyramidKV [8] allocates more memory in lower layers and less in higher ones, based on the empirical observation that the number of important tokens shrinks as the model depth increases, but still relies on static heuristics and cannot dynamically adjust cache allocations to suit various workloads. Complementary to KV cache pruning, another line of work [31, 49] addresses GPU memory constraints by offloading the entire KV cache to CPU memory and selectively loading important tokens to the GPU for attention computations. However, these methods do not inherently reduce the KV cache size and incur significant latency due to data transfers between the CPU and GPU.

3 MOTIVATION

In this section, we present the key findings that underpin the design of LeanKV, as well as their implications on KV cache management.

3.1 Impact of Key And Value

While the significance of different tokens can be directly inferred from attention scores, the roles of the key and value vectors within a token are less obvious. However, examining Equation 1 reveals a divergence in their impacts. Each token’s contribution to the attention output depends on two factors: the attention score from softmax and the value vector. Key vectors, as part of the shared softmax denominator, influence the attention scores of all tokens, whereas value vectors only affect their respective token’s contribution to the output.

Beyond the broader impact of key vectors, it is crucial to establish the *relative significance* of attention scores, determined by key vectors, over value vectors. Without this, the significance of key vectors could be overshadowed by that of value vectors. To this end, we reformulate the attention mechanism as a weighted sum of unit vectors, as presented in Equation 3. This formulation decomposes each input token’s contribution into two components: the unit vector $\frac{v_j}{|v_j|}$, representing only the direction of the token in feature space, and a coefficient, defined as the product of the attention score and the norm of the value vector, which determines the relative significance of the token’s direction. This allows us to assess the relative importance of attention scores and value vectors by examining their contributions to these coefficients.

$$\text{Attn}(\mathbf{Q}, \mathbf{K}, \mathbf{V})_i = \sum_{j=1}^i \underbrace{\text{softmax}\left(\frac{\mathbf{Q}\mathbf{K}^T}{\sqrt{d}}\right)_{ij}}_{\text{Coefficient}} \underbrace{|\mathbf{v}_j| \frac{\mathbf{v}_j}{|\mathbf{v}_j|}}_{\text{Unit vector}} \quad (3)$$

Figure 1 presents the distributions of the average attention score per token and the norms of value vectors across three representative layers of the Llama3-8B model [15], evaluated on the first one thousand articles from the Wikitext

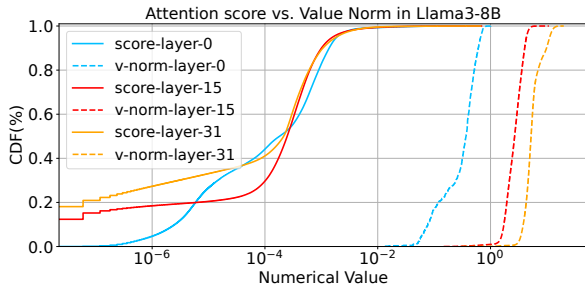


Figure 1: Distribution of attention score and value vector norm in Llama3-8B.

dataset [38]. Notably, the attention scores span seven orders of magnitude, vastly exceeding the range of value vector norms, which only cover at most two orders of magnitude. Similar patterns are also observed in the larger Llama3-70B model. This pronounced disparity highlights the pivotal role of attention scores in determining each token’s contribution to the attention output. We therefore conclude that key vectors exert a broader and more impactful influence than value vectors, motivating further exploration of processing key and value vectors at distinct precision levels.

3.2 Dynamic Sparsity Patterns

Existing approaches to KV cache pruning primarily rely on static memory allocation for each transformer layer in LLMs, either distributing memory uniformly [20, 32, 57, 62] or allocating it based on offline profiling [8]. However, LLMs exhibit dynamic sparsity patterns across both attention heads and individual requests, which static memory allocation cannot adequately handle. To evaluate the sparsity of attention computation, we analyze the minimum number of critical tokens required to retain the majority of information, specifically by preserving a target percentage (e.g., 95%) of the total attention score.

We begin by investigating dynamic sparsity patterns across layers. Using the first thousand articles from the Wikitext dataset, we evaluate the Llama3-8B model. Figure 2 illustrates the average number of critical tokens per layer, aggregated across all KV heads, required to retain 95% of the total attention score. Vertical bars represent the standard deviation, capturing variability across individual requests. Notably, the degree of sparsity varies considerably across layers, as indicated by differences in the number of critical tokens.

Next, we delve into the dynamic sparsity within individual layers. Figure 3 presents the average number of critical tokens per KV head for three representative layers, with horizontal bars indicating the standard deviation across requests. The sparsity pattern remains highly dynamic: within each layer, the number of critical tokens varies significantly across KV heads. Furthermore, within individual KV heads, the number of critical tokens can vary substantially across requests, as shown by the high standard deviation in some KV heads.

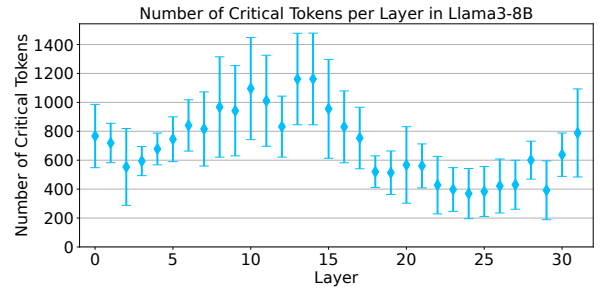


Figure 2: Number of critical tokens per layer in Llama3-8B to preserve 95% of the total attention score.

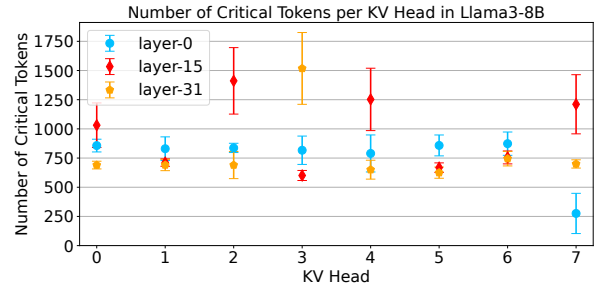


Figure 3: Number of critical tokens per KV head in Llama3-8B to preserve 95% of the total attention score.

These highly dynamic sparsity patterns, across layers, attention heads, and individual requests, underscore the necessity of adaptive memory management on a per-head and per-request basis.

3.3 Unifying Quantization and Pruning

Quantization compresses the KV cache by representing feature values with a reduced bit width, whereas pruning can be viewed as an extreme form of quantization: effectively storing feature values with zero bits. By using attention scores to measure the significance of tokens, we can unify the spectrum of KV cache compression by storing progressively less critical tokens at decreasing precision levels, ultimately leading to the pruning of the least critical tokens.

To investigate the feasibility of this unified approach, we experiment with a simple design: quantizing both the key and value vectors of significant tokens to 8 bits while pruning insignificant ones. Figure 4 compares the performance of the FP16 baseline, 8-bit quantization, pruning, and the combination of 8-bit quantization with pruning on the CNN/Daily Mail summarization dataset using the Llama3-8B model. For both pruning and the combined approach, approximately 20% of insignificant tokens are pruned. The ROUGE-1 score, which measures the fidelity of the LLM-generated responses to reference answers, is nearly indistinguishable among the four approaches. However, the combination of 8-bit quantization and pruning achieves the lowest memory usage. The improved efficiency of this combined approach motivates us to further

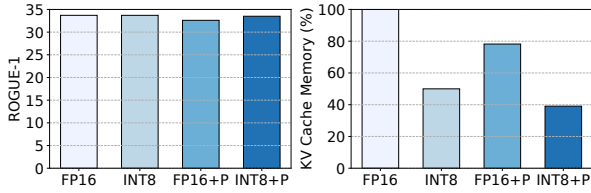


Figure 4: Rogue-1 score and normalized KV cache memory usage of the Llama3-8B model on CNN/DailyMail.

explore the spectrum of KV cache compression by introducing varying levels of precision to accommodate tokens of differing significance.

3.4 Key Findings and Implications

In this section, we outline the key findings that motivate the design of LeanKV. Specifically, we demonstrate that within individual tokens, key vectors have a greater impact than value vectors, inspiring us to propose storing key vectors at higher precision than value vectors. Beyond that, the significance of different tokens, as indicated by softmax scores, exhibits dynamic sparsity patterns across both heads and requests. These patterns necessitate flexible memory management on a per-head and per-request basis. Lastly, we show that unifying quantization and pruning can outperform either approach when used in isolation.

These findings motivate us to further explore the spectrum of KV cache compression, on a per-head and per-request basis to achieve the maximum memory efficiency. Specifically, each attention head should be allowed to store tokens at varying precision levels and to prune the least important ones, according to the sparsity patterns of individual requests. Additionally, within each token, the key and value vectors should be stored in different precisions. However, this unified approach presents significant challenges on memory management systems due to the resulting irregular memory layout, where the KV cache of each head and request consists of varying number of tokens stored at different precisions.

4 UNIFIED COMPRESSION ALGORITHM

In this section, we present the design of LeanKV’s unified compression algorithm, which leverages the insights from Section 3 to optimize memory efficiency. To account for the greater impact of key vectors compared to value vectors, we propose Hetero-KV, a strategy that quantizes keys at a higher precision than values. For instance, key and value vectors can be quantized to 8 and 4 bits (K8V4), or to 4 and 2 bits (K4V2). Additionally, we propose per-head memory management tailored to dynamic sparsity patterns. Rather than imposing a fixed memory budget, each head adaptively determines its memory allocation by quantizing tokens at various precision levels or pruning, based on the attention score distributions of individual requests. Specifically, tokens are categorized into three significance classes: the most important tokens are quantized at high precision (e.g., K8V4), moderately important

tokens at low precision (e.g., K4V2), and the least important tokens are pruned.

Next, we describe the unified compression algorithm in greater detail, addressing the prompt phase and the generation phase separately. Notably, in both phases, compression is conducted on a per-head and per-request basis.

Prompt Phase. In the prompt phase, key and value vectors for all tokens in the prompt are computed. The compression algorithm then determines the appropriate precision for storing each token based on its significance. The significance of the i^{th} token is calculated by averaging the $N - i$ attention scores it receives from subsequent tokens, where N denotes the sequence length. This average is then normalized to ensure that the total significance across all tokens sums to one.

To prevent premature compression, the algorithm reserves a recent window of size W , where all tokens are quantized at a high precision. W is predefined and typically set to 64. The remaining tokens are then sorted by significance. The least important N_p tokens, whose cumulative significance is below the threshold T_l , are pruned. The next N_l tokens, with a cumulative significance less than T_h , are quantized to low precision, while the most important N_h tokens are quantized to high precision. Here, $N_p + N_l + N_h + W = N$, and T_l and T_h are predefined thresholds determined by offline profiling. As a result of this mixed-precision compression, the KV cache is conceptually divided into two parts: a high precision section KV_h and a low precision section KV_l .

Generation Phase. In the generation phase, a single token is compressed at each step, aligning with the autoregressive nature of the generation process. The most recent token is added to the recent window to prevent premature compression, while the earliest token t_c in the window becomes a candidate for more aggressive compression. The compression procedure can be divided into two parts. First, token t_c is quantized at either a high or low precision and added to the corresponding section of the KV cache, or it may be completely pruned. Next, if t_c is quantized, the least significant token t_v in the corresponding precision section of the KV cache is either re-quantized to lower precision or pruned, depending on its significance. Essentially, this policy establishes a smooth downgrading path for the less important token: rather than being pruned directly, it is first re-quantized to low precision, with pruning occurring only if it remains insignificant.

The detailed procedure is outlined in Algorithm 1 and is governed by two predefined thresholds: the high precision threshold T_h and the low precision threshold T_l . If the significance of t_c is at least T_h , it is quantized at high precision and added to KV_h , the high precision section of the KV cache (line 6). Subsequently, the least significant token in KV_h is identified as the victim token t_v for more aggressive compression (line 7). If t_v ’s significance exceeds T_h , it remains in KV_h ; if it falls between T_h and T_l , t_v is re-quantized to low precision

and moved to KV_l , the low precision section of the KV cache (line 9); otherwise, t_v is pruned. Similarly, if t_c 's significance falls between T_h and T_l , it is quantized to low precision and added to KV_l (line 14). The least important token in KV_l is designated as the victim t_v (line 15), and is further pruned if its significance falls below T_l (line 17).

Notably, the proposed unified compression algorithm is extensible beyond three precision levels, and we adopt three precision levels to minimize metadata overhead and improve system efficiency, as detailed in the following section.

Algorithm 1: Unified compression (generation phase)

```

1: Input: Thresholds  $T_h$  &  $T_l$ ; Candidate token  $t_c$ 
2: Input: High & low precision  $P_h$  &  $P_l$ 
3: Input: High & low precision KV cache  $KV_h$  &  $KV_l$ 
4: Function: Significance Score; Quantization Quant;
5: if  $\text{Score}(t_c) \geq T_h$  then
6:    $KV_h.\text{add}(\text{Quant}(t_c, P_h))$ 
7:    $t_v = \text{argmin}_{t \in KV_h}(\text{Score}(t))$ 
8:   if  $T_l \leq \text{Score}(t_v) < T_h$  then
9:      $KV_h.\text{remove}(t_v), KV_l.\text{add}(\text{Quant}(t_v, P_l))$ 
10:  else if  $\text{Score}(t_v) < T_l$  then
11:     $KV_h.\text{remove}(t_v)$ 
12:  end if
13: else if  $\text{Score}(t_c) \geq T_l$  then
14:    $KV_l.\text{add}(\text{Quant}(t_c, P_l))$ 
15:    $t_v = \text{argmin}_{t \in KV_l}(\text{Score}(t))$ 
16:   if  $\text{Score}(t_v) < T_l$  then
17:      $KV_l.\text{remove}(t_v)$ 
18:   end if
19: end if

```

5 SYSTEM DESIGN

In this section, we present the design of the LeanKV system that leverages the proposed unified KV cache compression algorithm to boost LLM inference efficiency. We first discuss the challenges that the compression algorithm poses to system performance, and then present novel techniques to tackle these challenges.

5.1 Challenges

The Need for Flexible Paging. In PagedAttention [30], all tokens are stored at the same precision, making a fixed page format sufficient. However, Hetero-KV and mixed-precision quantization introduce varying precision levels across different tokens, rendering a fixed page format inadequate. Specifically, a fixed page format requires conservatively allocating high-precision slots for all tokens regardless of their actual precisions, leading to considerable memory wastage. Suppose memory is allocated to accommodate the highest precision K8V4, a token with K4V2 precision would waste 50% of the

memory. Additionally, such a fixed page format results in misaligned memory accesses, which hinder memory bandwidth utilization and reduce overall computational efficiency. To fully realize the benefits of Hetero-KV and mixed-precision quantization, we need a more flexible paging design that can dynamically adapt to varying precision levels, while ensuring compact memory usage and efficient memory accesses.

Increased Memory Management Overhead. The per-head KV cache compression algorithm in LeanKV introduces both significant latency and metadata overhead in memory management. In PagedAttention, the memory management complexity is $O(\#requests)$ regardless of the number of heads, as it partitions memory uniformly across heads and assigns identical page IDs to each head. In contrast, LeanKV must handle varying numbers of high-precision and low-precision tokens across different heads, which increases the complexity to $O(\#requests \times \#heads)$. If not carefully optimized, this overhead could overshadow the performance gains from cache compression. Moreover, to track both high-precision and low-precision tokens, a straightforward approach would involve using separate data structures for each precision, resulting in increased metadata overhead.

5.2 On-GPU Memory Management

A detailed analysis of the memory management process reveals opportunities for parallelization and acceleration. Specifically, memory management for the unified compression algorithm consists of two phases: *planning* and *coordination*. In the planning phase, each head independently determines its memory allocation requirements. The subsequent coordination phase synchronizes these per-head requirements and maps them to the GPU's physical memory. For instance, assume two attention heads require 16 and 32 bytes, respectively, as determined in the planning phase, with all GPU physical memory available. Then in the coordination phase, physical memory bytes 0 to 15 are allocated to the first head, and bytes 16 to 48 to the second. The primary source of increased memory management complexity lies in the planning phase, which is perfectly parallel and well-suited to the GPU's parallel compute capabilities. Parallelizing the coordination phase is more challenging, as it requires synchronization across heads. However, we observe that this phase can be parallelized effectively via parallel prefix sum [40].

Thus, we design an on-GPU memory management system to efficiently handle per-head dynamic memory allocation and recycling. This system introduces three GPU-resident data structures that collectively tackle the aforementioned challenges: the (1) *unified paging* to enable flexible paging, (2) the *circular free page list* to efficiently execute the coordination phase in memory management, and (3) the *bidirectional page table* to minimize metadata overhead for tracking high-precision and low-precision tokens.

Unified Paging. We partition the available GPU memory into evenly sized pages, each configured *upon allocation* to store tokens at a given precision. Each unified page consists of six segments: quantized keys, quantization metadata for keys, quantized values, quantization metadata for values, token scores, and positions. The quantization metadata includes scales and zero points for the key and value vectors. The number of tokens stored per page is adjusted according to the quantization configuration, ensuring compact memory usage. Unified paging allows flexible handling of tokens with varying precisions while maintaining a consistent memory layout, effectively supporting our unified compression algorithm. Furthermore, by consolidating keys, values, and their metadata into a single structure, unified paging enhances data locality and eliminates the need for scattered lookups, improving memory access efficiency during attention computation.

Circular Free Page List. To facilitate efficient page allocation and recycling, we manage all available page IDs in a centralized, GPU-resident data structure called *circular free page list*. The list tracks free pages using a pair of start and end pointers, which wrap to the beginning of the list upon reaching the end, maintaining a circular structure. When a page is allocated, the start pointer increments to the next available page ID; when a page is freed, the end pointer increments to add the freed page ID back to the list.

Notably, both the available and unavailable regions in the list remain contiguous, enabling the coordination phase in memory management to be parallelized via parallel prefix sum. Specifically, after each head determines the number of pages to be allocated or freed in the planning phase, a parallel prefix sum operation computes a unique offset for each head relative to the start or end pointer, ensuring non-conflicting operations within the list. For memory allocation, each head concurrently retrieves its new page IDs from its designated region in the list, with the start pointer incremented by the cumulative number of pages required across all heads. Similarly, for memory recycling, each head concurrently writes freed page IDs to its designated region, with the end pointer incremented by the total number of pages released.

Bidirectional Page Table. Similar to PagedAttention, LeanKV maintains a page table for each attention head, mapping requests to physical memory. Each entry in the page table is a list of page IDs allocated to the head for a specific request. To avoid the doubled metadata overhead associated with maintaining separate page tables for high- and low-precision pages, LeanKV introduces a unified, GPU-resident data structure called the *bidirectional page table*. This structure efficiently supports the use of three precision levels for KV cache compression, as proposed in Section 4, minimizing the metadata overhead. In each entry of the bidirectional page table, high-precision page IDs grow from the left side of the list, while low-precision page IDs grow from the right, dynamically

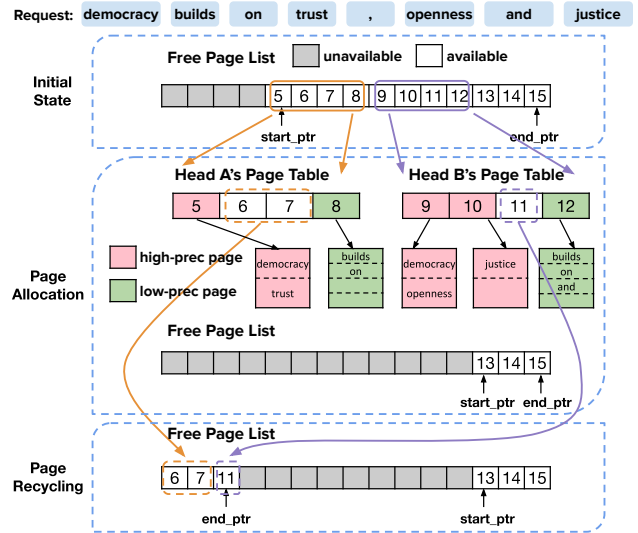


Figure 5: Memory management flow in the prompt phase.

adapting to the precision requirements of the workload. The length of each page table entry is determined by the maximum sequence length divided by the tokens per high-precision page, ensuring no overflow since low-precision pages always contain more tokens than high-precision ones. This unified approach not only minimizes metadata overhead but also eliminates the need for separate lookups based on precision levels, thereby enhancing memory access efficiency during attention computations. The memory overhead of the bidirectional page table is minimal: for example, with a batch size of 128 on Llama-2-7B, which has 32 layers and 32 attention heads per layer, the total size of all bidirectional page tables is only 64 MB. By contrast, the KV cache for a single request occupies 2 GB.

5.3 Memory Management Workflow

In this section, we delve into LeanKV’s memory management workflow, demonstrating how the proposed data structures interact to efficiently support unified KV cache compression. Notably, this memory management workflow is executed once per inference step for all requests in the batch and across all layers in the LLM. This design choice ensures sufficient parallelism for efficient GPU execution and amortizes the associated GPU kernel launch overheads.

Prompt Phase. Figure 5 illustrates the memory management workflow during the prompt phase using an example request with eight tokens. In this setting, one high-precision page can store two tokens, and one low-precision page can store four. Since the exact number of high- and low-precision pages required by each head is unknown prior to running the compression algorithm, we conservatively allocate four unified pages per head, assuming that all tokens will be stored at high precision. Each head then independently applies the KV cache compression algorithm to determine which tokens to

store at high-precision, low-precision, or to prune. This step constitutes the *planning phase*, during which each head calculates its specific memory needs based on its unique sparsity pattern. In this example, the first head uses one high-precision page, while the second head uses two; both heads also require one low-precision page. High-precision pages are allocated from the left side of the bidirectional page table, while low-precision pages are allocated from the right side. Following the planning phase, any unused pages are marked for recycling, triggering the *coordination phase*. Here, we employ a parallel prefix-sum-based approach, as described in the previous section, to facilitate efficient and conflict-free page recycling across heads.

Generation Phase. At each generation step, a head allocates a new page only if either its high-precision or low-precision pages are full, requiring at most one additional page per step. Each head independently checks its page availability and, if needed, allocates a new page in parallel using the prefix-sum-based approach. Unlike in the prompt phase, page recycling is not performed during generation, as the total number of stored tokens either remains the same if an old token is evicted or increases by one if no eviction occurs. Once a request is finished, all pages allocated for that request are recycled, freeing up memory for incoming requests.

6 IMPLEMENTATION

We implement LeanKV on top of vLLM, comprising 4.5K lines of CUDA/C++ code and 9K lines of Python. We first outline the architecture of LeanKV and then detail our custom GPU attention kernel, designed to efficiently support the unified cache compression algorithm.

6.1 LeanKV Architecture

The architecture of LeanKV is illustrated in Figure 6. At each inference step, the scheduler batches as many requests as possible within the available GPU memory to maximize throughput, sending the selected requests to all workers. Each GPU hosts one worker, responsible for executing a segment of the model. LeanKV utilizes tensor parallelism [51], where each worker handles a partition of each matrix multiplication and a subset of the attention heads. Each worker includes a dedicated memory manager to oversee the KV cache for its assigned attention heads, using the method described in Section 5. Due to dynamic sparsity patterns, memory requirements vary per head for each request, leading to an irregular memory layout. Additionally, each worker incorporates an execution engine for model computation. To support unified KV cache compression, the execution engine integrates a KV compressor and a custom GPU attention kernel. After computing key and value vectors, the KV compressor is invoked to compress them using the algorithm in Section 4, storing

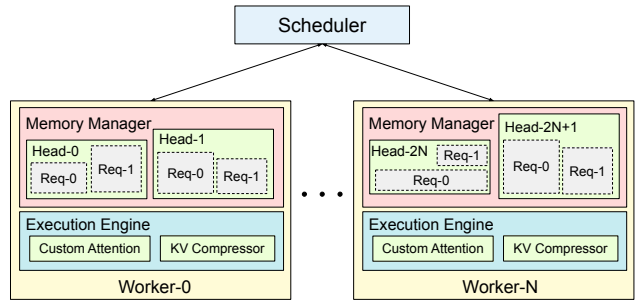


Figure 6: LeanKV architecture.

the results in the KV cache. The custom GPU attention kernel then efficiently computes the attention output using the compressed KV cache.

6.2 Efficient Attention Kernel

We develop a custom GPU attention kernel that efficiently supports per-head dynamic sparsity and Hetero-KV quantization, fully harnessing the reduction in memory access volume and translating it into accelerated performance.

Overall, we assign each CUDA thread block to process a single attention head per sequence. However, mixed-precision quantization introduces potential load imbalance, as high-precision tokens demand more bandwidth, which is the bottleneck of attention, than low-precision ones. Thanks to the unified paging mechanism that stores tokens of the same precision together in a page, we mitigate this issue by having thread warps iterate over high-precision pages first, followed by low-precision pages, ensuring that threads within a warp remain load-balanced. Each page is processed in two phases: dot product between the query and keys to derive attention scores, and weighted sum of values. These two phases follow different computation patterns: reduction over the feature dimension and token dimension, respectively. To ensure coalesced and vectorized memory accesses for both phases, we design tailored data layouts and parallelization strategies, elaborated in the following paragraphs.

For key processing, each warp handles one page at a time, with threads in the warp divided into groups responsible for distinct keys. Within a group, each thread fetches its assigned keys in a vectorized manner, performs dequantization on the fly, and computes a partial dot product between the keys and corresponding query. Using a straightforward layout such as $[F, N_{\text{tokens}}]$ for keys in each page, where F denotes the feature dimension length, would cause threads within a group to fetch non-contiguous elements strided by N_{tokens} when parallelizing across the feature dimension. Alternatively, using $[N_{\text{tokens}}, F]$ would cause thread groups to fetch non-contiguous elements strided by F when parallelizing across tokens. Both layouts suffer inefficient strided memory accesses, leading to low bandwidth utilization. Instead, we organize the layout of keys as $[\frac{F}{K_{\text{vec}} \times K_{\text{group}}}, N_{\text{tokens}}, K_{\text{group}}, K_{\text{vec}}]$, where K_{vec} denotes the

vectorization factor and K_{group} denotes the number of threads per group. During each execution step, each thread fetches K_{vec} consecutive elements, threads within a group collectively fetch K_{group} adjacent chunks, and groups within the warp access contiguous chunks along the N_{tokens} dimension. As a result, the combined memory accesses of all threads in a warp are contiguous, enabling memory coalescing and maximizing bandwidth utilization.

For value processing, tokens in a page are evenly distributed across thread groups in a warp; within each group, individual threads perform sum reductions over specific ranges of the feature dimension and save their accumulation results in registers. Once all groups finish, a tree reduction aggregates these partial results and produces the output. The number of registers required per thread is proportional to the feature dimension range assigned to it, while during key processing each thread only requires a single register to store the partial dot product. As a consequence, vectorization along the feature dimension, as used in key processing, is not suitable for value processing, because it would significantly increase register pressure by forcing each thread to handle a larger portion of the feature dimension. To better align with the computation pattern of reduction across tokens during value processing, we apply vectorization to the token dimension instead, which reduces register pressure and ensures more effective parallelization. We organize the layout of values as $[\frac{F}{V_{\text{group}}}, \frac{N_{\text{tokens}}}{V_{\text{vec}}}, V_{\text{group}}, V_{\text{vec}}]$ accordingly.

7 EVALUATION

We first evaluate the effectiveness of LeanKV’s unified KV cache compression algorithm and analyze the sensitivity of different models to KV cache compression. Then, We demonstrate the improvements in throughput achieved by LeanKV.

7.1 Experiment Setup

We evaluate LeanKV on six models across three families: Llama2-7B and 70B [54], Llama3-8B and 70B [15], Mistral-7B [27], and Mixtral-8x7B [28]. Mixtral-8x7B employs a Mixture-of-Experts (MOE) architecture, while the remaining models are dense. Performance of LeanKV is evaluated on five benchmarks, grouped into two categories. The first includes tasks requiring advanced reasoning and logic: GSM8K [11] (mathematics), HumanEval [9] (coding), and MMLU [25] (academic level question answering). The second category includes traditional text processing tasks: SQuAD [45] (reading comprehension) and CNN-DailyMail [41] (summarization). Throughput and latency is measured on Nvidia L40 GPUs, each with 48GB of memory [42].

7.2 Evaluating Unified Cache Compression

We first demonstrate the effectiveness of Hetero-KV quantization and dynamic sparsity individually, and then evaluate the

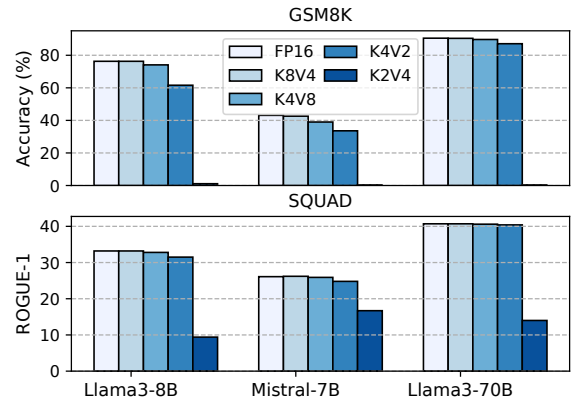


Figure 7: Performance of Hetero-KV.

end-to-end benefits of the proposed unified KV cache compression. To mitigate the noise and randomness in floating-point computations, each experiment is repeated five times with the dataset randomly shuffled, and the reported results are the average of these runs.

Evaluating Hetero-KV. Figure 7 shows the performance of Hetero-KV quantization, namely K8V4 and K4V2, compared to FP16 baselines, on GSM8K and SQuAD, representing benchmarks from the two categories. To validate our intuition that key vectors have a more significant impact than value vectors (Section 3.1), we additionally evaluate the mirror configurations of Hetero-KV, namely K4V8 and K2V4, where values are stored with higher precision than keys.

K8V4 maintains the accuracy of the FP16 baseline across both benchmarks for all models, whereas its mirror configuration, K4V8, results in noticeable degradation, particularly on the reasoning-intensive GSM8K benchmark. The performance gap between K4V2 and K2V4 is even more pronounced. On GSM8K, K4V2 retains at least 77.8% of FP16 performance, while K2V4 reduces accuracy to nearly zero for all models. On SQuAD, K4V2 achieves 94.7% to 99.4% of FP16 performance, whereas K2V4 achieves only 28.2% to 60.0%. These results confirm that key vectors play a more critical role than value vectors, and demonstrate that Hetero-KV is effective in maintaining the accuracy of the FP16 baseline.

Evaluating Dynamic Sparsity. We evaluate the effectiveness of per-head dynamic sparsity (Section 3.2) in identifying critical tokens, comparing it to the static sparsity method used in H2O [62], which allocates an equal memory budget to all attention heads. The results are shown in Figure 8, where we use the Mistral-7B model as an example and all tokens are stored in FP16.

For reasoning-intensive workloads such as GSM8K and HumanEval, dynamic sparsity significantly outperforms static sparsity, with the performance gap widening as the fraction of pruned tokens increases. For traditional text processing tasks, however, the benefits of dynamic sparsity are less pronounced:

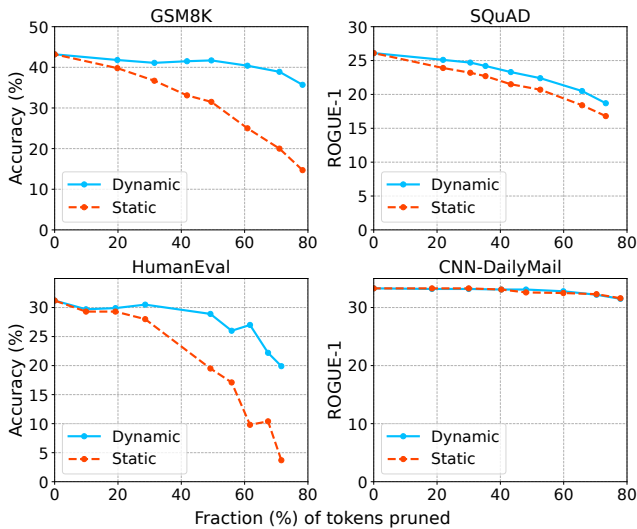


Figure 8: Performance of dynamic vs. static sparsity.

it slightly outperforms static sparsity on SQuAD and performs similarly on CNN-DailyMail.

The difference between SQuAD and CNN-DailyMail can be attributed to their differing sensitivities to token pruning. SQuAD (reading comprehension) requires precise retrieval of specific words from the prompt, making it more sensitive to pruning critical tokens. In contrast, CNN-DailyMail (summarization) inherently involves discarding less relevant information to generate concise summaries, resulting in lower sensitivity to token pruning. To summarize, dynamic sparsity is superior to static sparsity for reasoning-intensive tasks and text processing that involves precise information retrieval.

Evaluating Unified KV Cache Compression. Finally, we evaluate the end-to-end performance of the unified KV cache compression described in Section 4. For each benchmark, we perform grid search over the high-precision threshold T_h (with discrete values from $\{0.5\%, 1\%, 5\%, 10\%, 20\%\}$) and the low-precision threshold T_l (with discrete values from $\{0\%, 0.1\%, 0.5\%, 1\%\}$), selecting the configurations that minimize the KV cache memory budget under different performance constraints. To account for the inherent randomness in floating-point computations, we consider a configuration to be performance-neutral if its average performance falls within three standard deviations of the FP16 baseline.

Table 1 reports the KV cache memory usage of LeanKV, normalized to vLLM [30], across all evaluated models and benchmarks. The results are presented for two configurations: performance-neutral, which ensures no degradation in output quality, and less-than-5% performance degradation, a common target in prior work [17, 18, 31, 34, 35, 63] that enables more aggressive memory savings while preserving acceptable quality. Across models and workloads, LeanKV achieves performance neutral with 18.9% to 28.9% of the KV cache

memory budget, and less-than-5% performance degradation with 7.6% to 20.6% of the memory budget.

Additionally, Figure 9 shows the Pareto performance-memory curves of LeanKV on the reasoning-intensive benchmark GSM8K and text processing benchmark SQuAD. The results are compared against the FP16 baseline, conventional 8-bit quantization (K8V8) and 4-bit quantization (K4V4), and the pruning-only technique H2O [62]. For GSM8K, K8V8 preserves the FP16 baseline performance, while K4V4 leads to a noticeable performance degradation of 2.8% to 7.3%. In comparison, LeanKV achieves FP16-equivalent performance with only 19.8% to 23.1% of the memory budget, even less than K4V4, which requires 25% memory. Moreover, LeanKV offers a more flexible memory-performance tradeoff, with performance degradation limited to less than 5% while using just 9.4% to 16.3% of the memory. In contrast, under similar memory constraints, H2O results in near-zero accuracy. Similar trends are observed on the SQuAD benchmark: LeanKV matches the performance of FP16 and K8V8 with less memory than K4V4, which causes noticeable performance degradation, and outperforms H2O under comparable memory budgets.

Notably, across all evaluated models and benchmarks, LeanKV achieves performance-neutral with the K8V4-K4V2 configuration, where critical tokens are stored with K8V4 precision, non-critical tokens with K4V2, and no pruning is applied. For the less-than-5% degradation setting, the optimal configuration varies across models. For large 70B models, less-than-5% degradation is achieved with the more aggressive K4V2-K4V1 quantization without pruning, as pruning significantly degrades performance even on top of K8V4-K4V2. In contrast, for smaller models, less-than-5% degradation is achieved by further pruning the least important tokens on top of K8V4-K4V2. These varying configurations in low-memory regimes are also visualized in Figure 9, where each data point for LeanKV is annotated with its corresponding configuration. This disparity underscores the varying sensitivity of models to KV cache compression techniques, emphasizing the need for a unified framework capable of adapting to diverse scenarios to maximize efficiency.

In summary, LeanKV provides a superior performance-memory tradeoff compared to conventional methods. It maintains the performance of FP16 and 8-bit quantization while using even less memory than 4-bit quantization. Additionally, LeanKV offers a smooth tradeoff in the low-memory regime (10% to 20% of memory), where pruning-only methods experience significant performance degradation.

7.3 Sensitivity to KV Cache Compression

We investigate the varying sensitivity of models to KV cache compression, using the Llama model family as an example,

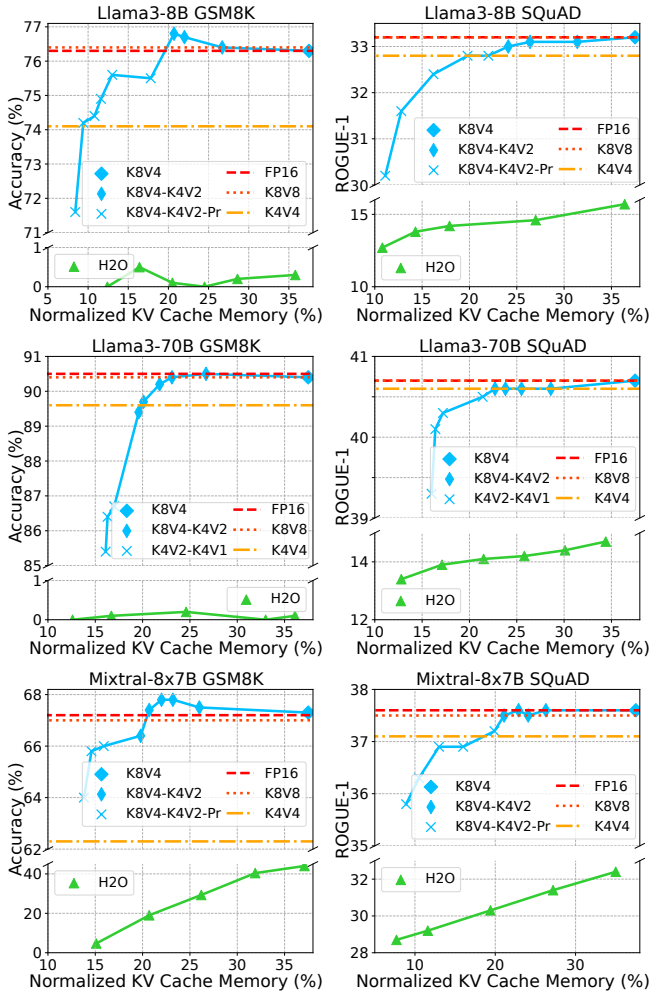


Figure 9: KV cache memory normalized to vLLM vs. benchmark performance tradeoff of LeanKV

Table 1: Memory usage of LeanKV normalized to vLLM across models and benchmarks.

Models		Benchmarks				
		GSM8K	MLLU	HumanEval	SQUAD	CNN-DailyMail
Llama2-7B	perf-neutral	18.9%	22.8%	23.1%	21.2%	21.6%
	5% perf-loss	11.3%	11.5%	18.9%	14.6%	7.6%
Llama2-70B	perf-neutral	21.3%	21.4%	21.2%	21.1%	20.1%
	5% perf-loss	19.5%	15.9%	18.2%	16.0%	15.7%
Llama3-8B	perf-neutral	20.7%	26.7%	26.6%	24.1%	20.0%
	5% perf-loss	9.4%	20.6%	22.1%	12.8%	8.8%
Llama3-70B	perf-neutral	23.1%	21.5%	22.7%	22.7%	19.5%
	5% perf-loss	16.3%	16.1%	21.2%	16.0%	15.7%
Mistral-7B	perf-neutral	26.8%	28.9%	23.0%	26.2%	19.4%
	5% perf-loss	17.7%	13.6%	15.1%	15.9%	9.7%
Mixtral-8x7B	perf-neutral	19.8%	20.1%	21.4%	21.1%	20.0%
	5% perf-loss	13.8%	8.9%	10.7%	8.9%	10.0%

due to their similar training data and methodologies. Figure 10 illustrates the normalized performance degradation relative to the FP16 baseline for Llama2-7B, Llama3-8B, and Llama3-70B as the fraction of pruned tokens increases. Among the models, Llama2-7B exhibits the least performance degradation, even when compared to Llama3-8B, which has

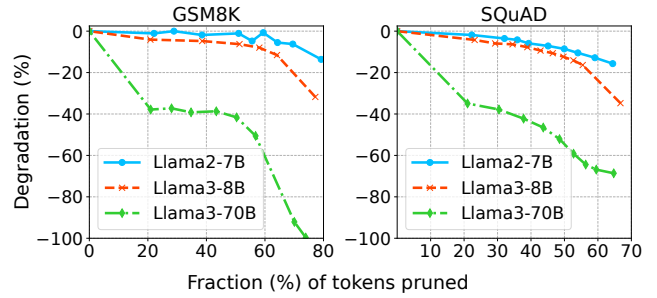


Figure 10: Sensitivity to KV cache pruning.

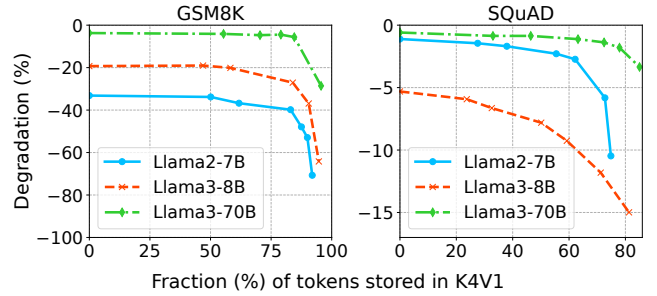


Figure 11: Sensitivity to low-bit KV cache quantization.

a comparable parameter size. This resilience can be attributed to Llama2-7B’s MHA architecture, which introduces greater redundancy in the KV cache compared to the more memory efficient GQA architecture utilized by Llama3-8B and Llama3-70B. Llama3-70B experiences the most significant performance degradation, suggesting that larger models distribute attention more evenly across tokens, making them more sensitive to pruning.

Figure 11 further illustrates the normalized performance degradation of the K4V2-K4V1 configuration as the fraction of tokens stored in K4V1 increases. The Llama3-70B model exhibits the greatest resilience to low-bit quantization, maintaining near-baseline performance even when 60% of tokens are stored in K4V1. In comparison, smaller models show noticeable performance degradation even when all tokens are stored in K4V2, highlighting their greater sensitivity to aggressive quantization.

These observations justify the two key trends outlined earlier: larger models and newer models employing more memory-efficient network architectures are more sensitive to pruning, while smaller models are more adversely impacted by low-bit quantization.

7.4 Evaluating Latency and Throughput

In this section, we provide a comprehensive evaluation of LeanKV’s performance, comparing it against state-of-the-art systems including vLLM and H2O across various models and configurations. All experiments were conducted on a machine equipped with eight NVIDIA L40 GPUs. For models that fit into a single GPU’s memory, such as Llama2-7B

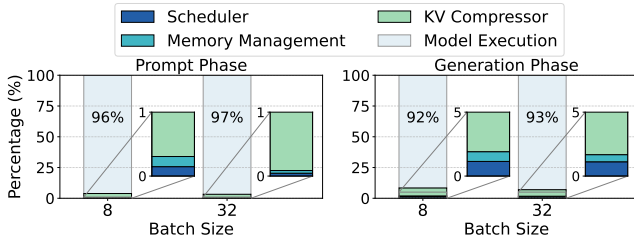


Figure 12: Latency breakdown of LeanKV.

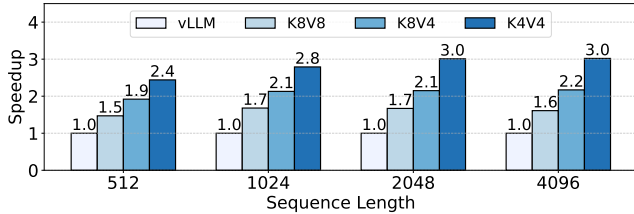


Figure 13: Attention kernel speedup.

and Llama3-7B, we use one GPU. For larger models like Llama2-70B and Llama3-70B, we parallelize the computation across four GPUs. Our evaluation focuses on latency breakdown, attention kernel speedup, and end-to-end throughput to demonstrate the efficiency and scalability of LeanKV. **Memory Management Overhead.** Figure 12 shows the latency breakdown of LeanKV during one inference step with a sequence length of 1024 tokens, evaluated across different batch sizes. The memory management overhead is remarkably low, contributing less than 0.2% of the total latency in the prompt phase and under 0.9% in the generation phase. Model execution dominates the latency in both phases, accounting for 96–97% of the latency in the prompt phase and 92–93% in the generation phase. Notably, as the batch size increases, the percentage of time spent on model execution rises slightly, reflecting the scalability of LeanKV. For comparison, in vLLM, model execution contributes 97% of the latency in the prompt phase and 95% in the generation phase. These results demonstrate that LeanKV effectively minimizes latency contributions from memory management and KV compression, ensuring that these auxiliary processes do not become performance bottlenecks.

Attention Kernel Speedup. Figure 13 shows the speedup of the LeanKV’s custom attention kernel against vLLM under different quantization configurations. LeanKV achieves a near-linear speedup proportional to the reduction in KV cache size. For example, with K8V8, which halves the KV cache size relative to FP16 datatype, the theoretical speedup is 2 \times , and LeanKV achieves 1.7 \times . The slight gap is primarily due to the overhead of accessing quantization metadata and performing dequantization. Additionally, LeanKV achieves greater speedups on longer sequences, indicating that its bandwidth optimization techniques become increasingly effective as the sequence length grows.

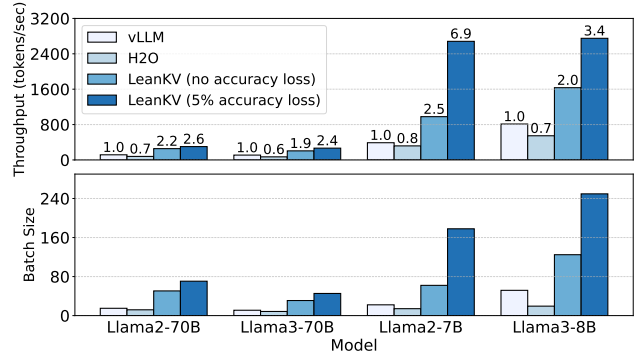


Figure 14: Throughput and achieved batch size.

End-to-End Throughput. Figure 14 presents the end-to-end throughput and achieved batch sizes of LeanKV compared to vLLM and H2O. We conduct experiments on 1000 sequences sampled from the ShareGPT [3] dataset, setting the generation length to 4096 tokens. The compression thresholds for LeanKV are selected based on the most challenging dataset, MMLU, making them the most conservative choices. In configurations with no accuracy loss, LeanKV achieves throughput speedups ranging from 2.0 \times to 2.5 \times compared to vLLM across various models. When allowing a 5% accuracy loss, LeanKV achieves even higher speedups, ranging from 3.0 \times to 6.9 \times . These improvements are directly correlated with the larger batch sizes supported by LeanKV, enabled by its KV cache compression techniques. For instance, with the Llama2-7B model, LeanKV sustains a batch size of 62 without accuracy loss and 177 with 5% accuracy loss, far exceeding vLLM’s batch size of 22. The increased batch size enables LeanKV to maximize the utilization of GPU compute capacity, leading to higher throughput. Llama3-7B exhibits a less significant speedup compared to Llama2-7B because it utilizes GQA, which reduces its KV cache size by 4 \times . As a result, vLLM already supports a relatively large batch size of 51.5 for Llama3-7B, narrowing the batch size advantage that LeanKV can leverage. Nevertheless, LeanKV still achieves up to 3.4 \times higher throughput over vLLM on Llama3-7B.

Notably, H2O supports even smaller batch sizes than vLLM and consequently has lower throughput. This is because H2O consumes additional memory during the prompt phase for intermediate results required to calculate compression metrics, limiting the batch size that can be supported. In contrast, we design a FlashAttention-compatible kernel using Triton, which avoids the additional memory overhead caused by intermediate results and achieves performance on par with vLLM.

8 CONCLUSION

We propose LeanKV, a unified KV cache compression framework designed to enhance LLM serving efficiency through three key techniques: Hetero-KV, per-head dynamic sparsity, and unified KV compression. To support these innovations, LeanKV incorporates system optimizations including unified

paging and on-GPU parallel memory management. Our experiments show that LeanKV achieves $1.9\times$ to $2.5\times$ higher throughput over state-of-the-art systems without compromising model accuracy, and up to $6.9\times$ higher throughput with minimal accuracy degradation.

REFERENCES

- [1] FasterTransformer. <https://github.com/NVIDIA/FasterTransformer>.
- [2] FlashInfer: Kernel Library for LLM Serving. <https://github.com/flashinfer-ai/flashinfer>.
- [3] ShareGPT. <https://sharegpt.com/>.
- [4] ACHIAM, J., ADLER, S., AGARWAL, S., AHMAD, L., AKKAYA, I., ALEMAN, F. L., ALMEIDA, D., ALTENSCHMIDT, J., ALTMAN, S., ANADKAT, S., ET AL. Gpt-4 technical report. *arXiv preprint arXiv:2303.08774* (2023).
- [5] AINSLIE, J., LEE-THORP, J., DE JONG, M., ZEMLYANSKIY, Y., LEBRÓN, F., AND SANGHAI, S. Gqa: Training generalized multi-query transformer models from multi-head checkpoints. *arXiv preprint arXiv:2305.13245* (2023).
- [6] AMINABADI, R. Y., RAJBHANDARI, S., AWAN, A. A., LI, C., LI, D., ZHENG, E., RUWASE, O., SMITH, S., ZHANG, M., RASLEY, J., ET AL. Deepspeed-inference: enabling efficient inference of transformer models at unprecedented scale. In *SC22: International Conference for High Performance Computing, Networking, Storage and Analysis* (2022), IEEE, pp. 1–15.
- [7] BROWN, T. B. Language models are few-shot learners. *arXiv preprint arXiv:2005.14165* (2020).
- [8] CAI, Z., ZHANG, Y., GAO, B., LIU, T., LU, K., XIONG, W., DONG, Y., CHANG, B., HU, J., AND XIAO, W. Pyramidkv: Dynamic kv cache compression based on pyramidal information funneling. *arXiv preprint arXiv:2406.02069* (2024).
- [9] CHEN, M., TWOREK, J., JUN, H., YUAN, Q., PINTO, H. P. D. O., KAPLAN, J., EDWARDS, H., BURDA, Y., JOSEPH, N., BROCKMAN, G., ET AL. Evaluating large language models trained on code. *arXiv preprint arXiv:2107.03374* (2021).
- [10] CHIANG, W.-L., ZHENG, L., SHENG, Y., ANGELOPOULOS, A. N., LI, T., LI, D., ZHANG, H., ZHU, B., JORDAN, M., GONZALEZ, J. E., ET AL. Chatbot arena: An open platform for evaluating llms by human preference. *arXiv preprint arXiv:2403.04132* (2024).
- [11] COBBE, K., KOSARAJU, V., BAVARIAN, M., CHEN, M., JUN, H., KAISER, L., PLAPPERT, M., TWOREK, J., HILTON, J., NAKANO, R., ET AL. Training verifiers to solve math word problems. *arXiv preprint arXiv:2110.14168* (2021).
- [12] DAO, T. Flashattention-2: Faster attention with better parallelism and work partitioning. *arXiv preprint arXiv:2307.08691* (2023).
- [13] DAO, T., FU, D., ERMON, S., RUDRA, A., AND RÉ, C. Flashattention: Fast and memory-efficient exact attention with io-awareness. *Advances in Neural Information Processing Systems* 35 (2022), 16344–16359.
- [14] DETTMERS, T., LEWIS, M., BELKADA, Y., AND ZETTLEMOYER, L. Gpt3. int8 (): 8-bit matrix multiplication for transformers at scale. *Advances in Neural Information Processing Systems* 35 (2022), 30318–30332.
- [15] DUBEY, A., JAUHRI, A., PANDEY, A., KADIAN, A., AL-DAHLE, A., LETMAN, A., MATHUR, A., SCHELLEN, A., YANG, A., FAN, A., ET AL. The llama 3 herd of models. *arXiv preprint arXiv:2407.21783* (2024).
- [16] FANG, J., YU, Y., ZHAO, C., AND ZHOU, J. Turbotransformers: an efficient gpu serving system for transformer models. In *Proceedings of the 26th ACM SIGPLAN Symposium on Principles and Practice of Parallel Programming* (2021), pp. 389–402.
- [17] FRANTAR, E., AND ALISTARH, D. Sparsegpt: Massive language models can be accurately pruned in one-shot. In *International Conference on Machine Learning* (2023), PMLR, pp. 10323–10337.
- [18] FU, T., HUANG, H., NING, X., ZHANG, G., CHEN, B., WU, T., WANG, H., HUANG, Z., LI, S., YAN, S., ET AL. Moa: Mixture of sparse attention for automatic large language model compression. *arXiv preprint arXiv:2406.14909* (2024).
- [19] GAO, P., YU, L., WU, Y., AND LI, J. Low latency rnn inference with cellular batching. In *Proceedings of the Thirteenth EuroSys Conference* (2018), pp. 1–15.
- [20] GE, S., ZHANG, Y., LIU, L., ZHANG, M., HAN, J., AND GAO, J. Model tells you what to discard: Adaptive kv cache compression for llms. *arXiv preprint arXiv:2310.01801* (2023).
- [21] GITHUB. Github copilot. <https://github.com/features/copilot>, 2023.
- [22] GUO, C., TANG, J., HU, W., LENG, J., ZHANG, C., YANG, F., LIU, Y., GUO, M., AND ZHU, Y. Olive: Accelerating large language models via hardware-friendly outlier-victim pair quantization. In *Proceedings of the 50th Annual International Symposium on Computer Architecture* (2023), pp. 1–15.
- [23] GUO, D., ZHU, Q., YANG, D., XIE, Z., DONG, K., ZHANG, W., CHEN, G., BI, X., WU, Y., LI, Y., ET AL. Deepseek-coder: When the large language model meets programming—the rise of code intelligence. *arXiv preprint arXiv:2401.14196* (2024).
- [24] HAN, M., ZHANG, H., CHEN, R., AND CHEN, H. Microsecond-scale preemption for concurrent {GPU-accelerated}{DNN} inferences. In *16th USENIX Symposium on Operating Systems Design and Implementation (OSDI 22)* (2022), pp. 539–558.
- [25] HENDRYCKS, D., BURNS, C., BASART, S., ZOU, A., MAZEIKA, M., SONG, D., AND STEINHARDT, J. Measuring massive multitask language understanding. *arXiv preprint arXiv:2009.03300* (2020).
- [26] HOOPER, C., KIM, S., MOHAMMADZADEH, H., MAHONEY, M. W., SHAO, Y. S., KEUTZER, K., AND GHOLAMI, A. Kvquant: Towards 10 million context length llm inference with kv cache quantization. *arXiv preprint arXiv:2401.18079* (2024).
- [27] JIANG, A. Q., SABLAYROLLES, A., MENSCH, A., BAMFORD, C., CHAPLOT, D. S., CASAS, D. D. L., BRESSAND, F., LENGYEL, G., LAMPLE, G., SAULNIER, L., ET AL. Mistral 7b. *arXiv preprint arXiv:2310.06825* (2023).
- [28] JIANG, A. Q., SABLAYROLLES, A., ROUX, A., MENSCH, A., SAVARY, B., BAMFORD, C., CHAPLOT, D. S., CASAS, D. D. L., HANNA, E. B., BRESSAND, F., ET AL. Mixtral of experts. *arXiv preprint arXiv:2401.04088* (2024).
- [29] KAO, S.-C., SUBRAMANIAN, S., AGRAWAL, G., YAZDANBAKHSH, A., AND KRISHNA, T. Flat: An optimized dataflow for mitigating attention bottlenecks. In *Proceedings of the 28th ACM International Conference on Architectural Support for Programming Languages and Operating Systems, Volume 2* (2023), pp. 295–310.
- [30] KWON, W., LI, Z., ZHUANG, S., SHENG, Y., ZHENG, L., YU, C. H., GONZALEZ, J., ZHANG, H., AND STOICA, I. Efficient memory management for large language model serving with pagedattention. In *Proceedings of the 29th Symposium on Operating Systems Principles* (2023), pp. 611–626.
- [31] LEE, W., LEE, J., SEO, J., AND SIM, J. {InfiniGen}: Efficient generative inference of large language models with dynamic {KV} cache management. In *18th USENIX Symposium on Operating Systems Design and Implementation (OSDI 24)* (2024), pp. 155–172.
- [32] LI, Y., HUANG, Y., YANG, B., VENKITESH, B., LOCATELLI, A., YE, H., CAI, T., LEWIS, P., AND CHEN, D. Snapkv: Llm knows what you are looking for before generation. *arXiv preprint arXiv:2404.14469* (2024).
- [33] LI, Z., ZHENG, L., ZHONG, Y., LIU, V., SHENG, Y., JIN, X., HUANG, Y., CHEN, Z., ZHANG, H., GONZALEZ, J. E., ET AL. {AlpaServe}:

- Statistical multiplexing with model parallelism for deep learning serving. In *17th USENIX Symposium on Operating Systems Design and Implementation (OSDI 23)* (2023), pp. 663–679.
- [34] LIN, J., TANG, J., TANG, H., YANG, S., CHEN, W.-M., WANG, W.-C., XIAO, G., DANG, X., GAN, C., AND HAN, S. Awq: Activation-aware weight quantization for on-device llm compression and acceleration. *Proceedings of Machine Learning and Systems 6* (2024), 87–100.
- [35] LIN, Y., TANG, H., YANG, S., ZHANG, Z., XIAO, G., GAN, C., AND HAN, S. Qserve: W4a8kv4 quantization and system co-design for efficient llm serving. *arXiv preprint arXiv:2405.04532* (2024).
- [36] LIU, A., FENG, B., WANG, B., WANG, B., LIU, B., ZHAO, C., DENG, C., RUAN, C., DAI, D., GUO, D., ET AL. Deepseek-v2: A strong, economical, and efficient mixture-of-experts language model. *arXiv preprint arXiv:2405.04434* (2024).
- [37] LIU, Z., DESAI, A., LIAO, F., WANG, W., XIE, V., XU, Z., KYRILIDIS, A., AND SHRIVASTAVA, A. Scissorhands: Exploiting the persistence of importance hypothesis for llm kv cache compression at test time. *Advances in Neural Information Processing Systems 36* (2024).
- [38] MERITY, S., XIONG, C., BRADBURY, J., AND SOCHER, R. Pointer sentinel mixture models. *arXiv preprint arXiv:1609.07843* (2016).
- [39] NAGEL, M., FOURNARAKIS, M., AMJAD, R. A., BONDARENKO, Y., VAN BAALLEN, M., AND BLANKEVOORT, T. A white paper on neural network quantization. *arXiv preprint arXiv:2106.08295* (2021).
- [40] NAKANO, K. An optimal parallel prefix-sums algorithm on the memory machine models for gpus. In *International Conference on Algorithms and Architectures for Parallel Processing* (2012), Springer, pp. 99–113.
- [41] NALLAPATI, R., ZHOU, B., GULCEHRE, C., XIANG, B., ET AL. Abstractive text summarization using sequence-to-sequence rnns and beyond. *arXiv preprint arXiv:1602.06023* (2016).
- [42] NVIDIA. Nvidia l40 datasheet. <https://www.nvidia.com/content/dam/en-zz/Solutions/design-visualization/support-guide/NVIDIA-L40-Datasheet-January-2023.pdf>, 2023.
- [43] OUYANG, L., WU, J., JIANG, X., ALMEIDA, D., WAINWRIGHT, C., MISHKIN, P., ZHANG, C., AGARWAL, S., SLAMA, K., RAY, A., ET AL. Training language models to follow instructions with human feedback. *Advances in neural information processing systems 35* (2022), 27730–27744.
- [44] POPE, R., DOUGLAS, S., CHOWDHERY, A., DEVLIN, J., BRADBURY, J., HEER, J., XIAO, K., AGRAWAL, S., AND DEAN, J. Efficiently scaling transformer inference. *Proceedings of Machine Learning and Systems 5* (2023), 606–624.
- [45] RAJPURKAR, P., JIA, R., AND LIANG, P. Know what you don’t know: Unanswerable questions for squad. *arXiv preprint arXiv:1806.03822* (2018).
- [46] SAAB, K., TU, T., WENG, W.-H., TANNO, R., STUTZ, D., WULCZYN, E., ZHANG, F., STROTHER, T., PARK, C., VEDADI, E., ET AL. Capabilities of gemini models in medicine. *arXiv preprint arXiv:2404.18416* (2024).
- [47] SHAO, Z., WANG, P., ZHU, Q., XU, R., SONG, J., ZHANG, M., LI, Y., WU, Y., AND GUO, D. Deepseekmath: Pushing the limits of mathematical reasoning in open language models. *arXiv preprint arXiv:2402.03300* (2024).
- [48] SHAZEER, N. Fast transformer decoding: One write-head is all you need. *arXiv preprint arXiv:1911.02150* (2019).
- [49] SHENG, Y., ZHENG, L., YUAN, B., LI, Z., RYABININ, M., CHEN, B., LIANG, P., RÉ, C., STOICA, I., AND ZHANG, C. Flexgen: High-throughput generative inference of large language models with a single gpu. In *International Conference on Machine Learning* (2023), PMLR, pp. 31094–31116.
- [50] SHI, Y., YANG, Z., XUE, J., MA, L., XIA, Y., MIAO, Z., GUO, Y., YANG, F., AND ZHOU, L. Welder: Scheduling deep learning memory access via tile-graph. In *17th USENIX Symposium on Operating Systems Design and Implementation (OSDI 23)* (2023), pp. 701–718.
- [51] SHOEYBI, M., PATWARY, M., PURI, R., LEGRSLEY, P., CASPER, J., AND CATANZARO, B. Megatron-llm: Training multi-billion parameter language models using model parallelism. *arXiv preprint arXiv:1909.08053* (2019).
- [52] TEAM, G., ANIL, R., BORGEAUD, S., WU, Y., ALAYRAC, J.-B., YU, J., SORICUT, R., SCHALKWYK, J., DAI, A. M., HAUTH, A., ET AL. Gemini: a family of highly capable multimodal models. *arXiv preprint arXiv:2312.11805* (2023).
- [53] TEAM, T. V. Vicuna: An open-source chatbot impressing gpt-4 with 90
- [54] TOUVRON, H., MARTIN, L., STONE, K., ALBERT, P., ALMAHAIRI, A., BABAEI, Y., BASHLYKOV, N., BATRA, S., BHARGAVA, P., BHOSALE, S., ET AL. Llama 2: Open foundation and fine-tuned chat models. *arXiv preprint arXiv:2307.09288* (2023).
- [55] VASWANI, A. Attention is all you need. *Advances in Neural Information Processing Systems* (2017).
- [56] WOLF, T., DEBUT, L., SANH, V., CHAUMOND, J., DELANGUE, C., MOI, A., CISTAC, P., RAULT, T., LOUF, R., FUNTOWICZ, M., ET AL. Transformers: State-of-the-art natural language processing. In *Proceedings of the 2020 conference on empirical methods in natural language processing: system demonstrations* (2020), pp. 38–45.
- [57] XIAO, G., TIAN, Y., CHEN, B., HAN, S., AND LEWIS, M. Efficient streaming language models with attention sinks. *arXiv preprint arXiv:2309.17453* (2023).
- [58] XIE, Y., WU, J., TU, H., YANG, S., ZHAO, B., ZONG, Y., JIN, Q., XIE, C., AND ZHOU, Y. A preliminary study of o1 in medicine: Are we closer to an ai doctor? *arXiv preprint arXiv:2409.15277* (2024).
- [59] YANG, Y., ZHAO, L., LI, Y., ZHANG, H., LI, J., ZHAO, M., CHEN, X., AND LI, K. Influx: a native serverless system for low-latency, high-throughput inference. In *Proceedings of the 27th ACM International Conference on Architectural Support for Programming Languages and Operating Systems* (2022), pp. 768–781.
- [60] YU, G.-I., JEONG, J. S., KIM, G.-W., KIM, S., AND CHUN, B.-G. Orca: A distributed serving system for {Transformer-Based} generative models. In *16th USENIX Symposium on Operating Systems Design and Implementation (OSDI 22)* (2022), pp. 521–538.
- [61] ZHANG, H., TANG, Y., KHANDELWAL, A., AND STOICA, I. {SHEPHERD}: Serving {DNNs} in the wild. In *20th USENIX Symposium on Networked Systems Design and Implementation (NSDI 23)* (2023), pp. 787–808.
- [62] ZHANG, Z., SHENG, Y., ZHOU, T., CHEN, T., ZHENG, L., CAI, R., SONG, Z., TIAN, Y., RÉ, C., BARRETT, C., ET AL. H2o: Heavy-hitter oracle for efficient generative inference of large language models. *Advances in Neural Information Processing Systems 36* (2024).
- [63] ZHAO, Y., LIN, C.-Y., ZHU, K., YE, Z., CHEN, L., ZHENG, S., CEZE, L., KRISHNAMURTHY, A., CHEN, T., AND KASIKCI, B. Atom: Low-bit quantization for efficient and accurate llm serving. *Proceedings of Machine Learning and Systems 6* (2024), 196–209.
- [64] ZHONG, T., LIU, Z., PAN, Y., ZHANG, Y., ZHOU, Y., LIANG, S., WU, Z., LYU, Y., SHU, P., YU, X., ET AL. Evaluation of openai o1: Opportunities and challenges of agi. *arXiv preprint arXiv:2409.18486* (2024).